

Preparation and Characterization of Sol-gel Silica-modified Kenaf Bast Microfiber/Polypropylene Composites

Muzafar Zulkifli,^{a,*} Md. Sohrab Hossain,^{a,b,*} Nor Afifah Khalil,^b Ahmad Naim Ahmad Yahaya,^{a,b} Fahmi Asyadi Md Yusof,^a and Azanam Shah Hashim^{a,b}

The present study was conducted to determine the influence of the chemically modified kenaf bast fiber (KBF) on the mechanical, morphological, and thermal properties of fiber-reinforced polypropylene composites. The KBF was modified *via* the *in situ* sol-gel silica process through soaking the KBF in tetraethyl orthosilicate (TEOS) at a pH of 11, room temperature ($25\text{ }^{\circ}\text{C} \pm 1\text{ }^{\circ}\text{C}$), and a KBF to TEOS ratio of 1:10 for 24 h. Silica successfully formed on the surface of the KBF. Subsequently, the sol-gel silica-modified KBF was utilized to produce sol-gel silica-modified KBF-reinforced polypropylene (PP-KBF-S) composites. Several analytical methods were utilized to determine the mechanical, morphological, and thermal properties of the PP-KBF-S composites, which were then compared with those of the untreated KBF-reinforced polypropylene composite. The findings revealed that sol-gel silica modification of the KBF reduced the void content and enhanced the mechanical properties and thermal stability of the PP-KBF-S.

Keywords: Chemical modification; Sol-gel silica; Kenaf bast fiber; Polypropylene composite

Contact information: a: Universiti Kuala Lumpur-Malaysian Institute of Chemical and Bioengineering Technology, Lot 1988, Taboh Naning, 78000 Alor Gajah Melaka, Malaysia; b: Green Chemistry & Sustainable Technology Cluster, Universiti Kuala Lumpur-Malaysian Institute of Chemical and Bioengineering Technology, Lot 1988, Taboh Naning, 78000 Alor Gajah Melaka, Malaysia; c: School of Industrial Technology, Universiti Sains Malaysia. 118000 Penang, Malaysia;

* Corresponding author: muzafar@unikl.edu.my (M.Zulkifli); mdsohrab@unik.edu.my (M.S.Hossain)

INTRODUCTION

The increasing demand for biocomposites in numerous applications, including buildings, consumer products, and automobiles, has triggered extensive research and investment, especially in the US, Europe, and Japan (Lambert and Gupta 2004; Bismarck *et al.* 2006). The advantages in terms of the price, weight reduction, and marketing strategy have resulted in kenaf fiber-based composites being seen as a potentially direct alternative to synthetic fiber-based composites. Kenaf fiber can be used as a reinforcing filler for composites in several areas, such as automotive components and construction. Kenaf bast fiber (KBF) consists of cellulose, hemicellulose, and lignin. It is mainly composed of an amorphous matrix of hemicellulose and lignin that contains cellulose microfibrils (Davoudpour *et al.* 2015). The amorphous matrix is also made of pectin, fat, and wax. Cellulose is considered the main component of kenaf fibers. The cellulose consists of anhydro-D-glucose in polar linear condensation polymers, which contains three hydroxyl (-OH) groups. It is easily hydrolyzed by an acid, but resistant to oxidizing agents and alkali treatment (Abdul Khalil *et al.* 2016).

The KBF has been widely used to produce natural fiber-reinforced polymeric composites (Thakur and Thakur 2014; Davoudpour *et al.* 2015; Saba *et al.* 2015). However, the hydrophilicity of the lignocellulosic fibers results in poor compatibility with the thermoplastics matrix due to its hydrophobic nature. This causes the formed composites to have poor physical, mechanical, and thermal properties. Many researchers have done extensive research on improving the physicochemical and thermal properties of natural fiber composites by either a mechanical approach or chemical modification (Bismarck *et al.* 2006; Ireana Yusra *et al.* 2015; Saba *et al.* 2015; Owolabi *et al.* 2017; Rosamah *et al.* 2017). Yang *et al.* (2011) studied the effect of the filler loading on the mechanical properties when using untreated and chemically-modified natural fibers in polypropylene (PP) composites. It was found that the fiber size and alkali treatment influenced the mechanical properties of the composite. Bourmaud and Baley (2007) studied the mechanical, rheological, and thermal properties of reprocessed PP/hemp and PP/jute fiber composites. The results of their study indicated that reprocessing the fiber reduced the fiber length because of mechanical grinding and the injection action.

Because of the naturally ductile characteristics of PP, the introduction of more natural fibers might reduce the strength by creating areas of concentrated stress and reduce the strain at break. Tawakkal *et al.* (2014) found that the addition of KBF in the PP matrix did not cause a reduction in the tensile modulus and strength, and maintained the strain at break of the composite. This was also supported by Saad (2012), who observed that the addition of natural fibers to PP composites resulted in greater tensile properties compared with neat PP because of a better compatibility factor. To overcome the shortcomings of polypropylene-kenaf bast fiber (PP-KBF) composites, various studies have been conducted, especially using various chemical modifications of KBF. The most common methods reported in the literature are an alkali treatment, the addition of coupling agents or compatibilizers, and acetylation to either enhance the surface of the kenaf fiber or prepare a “bridge” connecting the hydrophilic kenaf to the hydrophobic thermoplastic (Ikeda and Kameda 2004; Hubbe *et al.* 2015; Abdul Khalil *et al.* 2016). The chemical modification process is usually performed by using functional groups obtained from the reagent that are capable of bonding to the natural fibers *via* existing hydroxyl groups (Saad 2012; Hubbe *et al.* 2015).

In recent years, lignocellulosic fiber that has been chemically modified *via* the *in situ* sol-gel silica process has gained popularity for use as a reinforcement filler in polymeric composites. Sol-gel silica allows for a better dispersion of fibers and enhances the physical properties of composites because *in situ* polymerization of tetraethyl orthosilicate (TEOS) in the polymeric network creates a homogeneous morphology (Bounor-Legaré and Cassagnau 2014). Synthesis of silica using the sol-gel process utilizes the reaction of silicon alkoxides as a precursor with water or ethanol as a solvent. The reaction takes place in the presence of a suitable catalyst with acidic or basic conditions. The simplest and most commonly used silica precursors are tetramethoxysilane (TMOS) and TEOS. The precursor is the source of silica, and water acts as a reactant to help join the alkoxide molecules together. The chemical reaction speed depends on the type of catalyst used, such as butylamine, ammonium hydroxide, and fluoride. Ikeda and Kameda (2004) successfully conducted an *in situ* sol-gel reaction using TEOS with up to 70 phr (per hundred rubber) of silica particles in 1,4 polyisoprene and increased in catalyst usage. The dispersion was found to be more homogenous and increased the tensile strength. A remarkable improvement was also observed in the

degree of strain-induced crystallization using wide-angle X-ray diffraction (XRD) analysis.

Although numerous studies have been conducted on the chemical modification of lignocellulosic fiber using the sol-gel silica process, a limited number of studies have been conducted on the isolation of sol-gel silica-modified KBF-reinforced polypropylene (PP-KBF-S) composites. Therefore, the present study isolated and characterized the PP-KBF-S composite. Additionally, the mechanical, morphological, and thermal properties of the PP-KBF-S composite were compared with that of the untreated KBF-reinforced polypropylene (PP-KBF) composite.

EXPERIMENTAL

Materials

The KBF was procured from Kenaf Natural Fiber Industries Sdn Bhd (Terengganu, Malaysia). Extrusion-grade PP (PP-MY302) was purchased from Polypropylene Malaysia Sdn Bhd (Pahang, Malaysia). The TEOS was purchased from Acros Organics-Thermo Fisher Scientific (Springfield, New Jersey, USA). Butylamine, which acted as part of the catalyst used in the sol-gel process, was obtained from Merck Millipore International (Selangor, Malaysia). All of the other chemicals used in this study were of analytical grade and purchased from Sigma-Aldrich (St. Louis, MO, USA).

Sample preparation

The KBF was obtained in the form of long fibers that were between 3 mm and 5 mm in length. The KBF was further refined to lengths of 300 μm to 500 μm using a disc mill at constant speed of 470 rpm for 2 min (model FFC-45 A, Qingdao Dahlia Double Circle Machinery Co., Ltd., (Qingdao, China). The KBF was then sieved in a shaker three consecutive times at 8 amps for 5 min to ensure a length of 300 μm to 500 μm .

In situ sol-gel silica process

The KBF was initially soaked in a butylamine solution at a pH of 11 for 4 h, and it was subsequently oven-dried at 110 $^{\circ}\text{C}$ for 6 h. The dried KBF was then soaked for 24 h in TEOS at a pH of 11, room temperature (25 $^{\circ}\text{C} \pm 1$ $^{\circ}\text{C}$), and a KBF to TEOS ratio of 1:10 gmL^{-1} . Later, the TEOS-treated KBF was separated by filtration and re-soaked in a butylamine solution at a pH of 11 and 40 $^{\circ}\text{C}$ for 1 h. It was subsequently oven-dried at 110 $^{\circ}\text{C}$ for another 6 h. It has been reported that the optimal pH for the sol-gel silica process is 11 (Hashim *et al.* 1995). The pH of the solution was controlled using concentrated sodium hydroxide (NaOH) and hydrogen chloride (HCl) solutions. The sol-gel silica-modified KBF (KBF-S) was then stored in a desiccator. The silica content (SC, %) in the KBF-S was calculated by the following equation:

$$\text{Silica content (\%)} = \frac{W_2 - W_1}{W_2} \times 100 \quad (1)$$

where W_1 is the weight of KBF (g) and W_2 is the weight of KBF-S (g).

Preparation of polypropylene composites with modified (PP-KBF-S) and unmodified kenaf bast fiber (PP-KBF)

The composite was prepared with KBF and KBF-S via a melt-blended process that was followed by a compression molding process. The process of melt blending was performed using a Thermo HAAKE 600 internal mixer (Victoria, Australia). The melt blending process was conducted by mixing 30 g of KBF and KBF-S with 70 g of PP at 175 °C and a rotor speed of 40 rpm with pre-heat and mixing times of 15 min (Tajeddin *et al.* 2010). The stabilization of the torque indicated the completion of the blending. The blended compound was then crunched into pellet form. The model of the cruncher machine used was AME-30p (Henan Yuhong Heavy Machinery Co., Ltd., Dalian, China). Crunching was crucial as compounds in a smaller pellet form provide the larger contact area needed in the compression molding process. Compression molding was the final step to produce the PP-KBF and PP-KBF-S composites, which was performed using a cold compression molding machine (model 4129-039, DOUSH, Shanghai, China).

Physical properties test

The burn test was performed according to ASTM D 3171 (2004) to determine the weight loss difference of the KBF and KBF-S. The samples was first burned in a Thermo Scientific Muffle Furnace under O₂ condition at 600 °C for 6 h. Then, the crucibles of the samples was cooled at room temperature in the desiccator and the weight was recorded. The sample was expressed as a percentage weight loss (%). The sample weight was approximately 5 g. The burn test identified and established the presence of silica in the specimen by the total burn off of the specimen (McDonough 2004). The measurement of composites density was conducted by following the ASTM D792 (2008). The void content was determined using ASTM D-2734 (2009), as below,

$$\text{Void content (\%)} = \frac{T_d - M_d}{T_d} \times 100 \quad (2)$$

where T_d is the theoretical composite density and M_d is the measured composite density. However, T_d can be calculated by following the Eq. 3.

$$T_d (\text{g} \cdot \text{cm}^{-3}) = \frac{1}{\left(\frac{w_f}{\rho_f} + \frac{w_m}{\rho_m}\right)} \quad (3)$$

where w_f is the weight fraction of fiber, ρ_f is the fiber density, w_m is the weight fraction of the matrix, and ρ_m is the matrix density.

Mechanical properties analyses

The tensile strength and the flexural strength of the prepared samples were evaluated according to ASTM D3039 (2014) and ASTM D790 (2015), respectively. The test was conducted using a Lloyds Universal Testing Machine (Lloyd Instruments Ltd., West Sussex, UK) with a strain rate of 2 mm/min. According to the standard, a minimum of five specimens were needed. The samples were conditioned for 2 d and the test was conducted at 23 °C ± 2 °C and 50% ± 5% relative humidity (RH).

The impact test was conducted on the prepared samples according to the ISO 179 (2010) standard using a Ray Ran Pendulum Impact Tester System (Warwickshire, UK) with a hammer weight of 1.189 kg. The velocity used was 2.9 m/s. The test was performed with a minimum of five samples that had the dimensions 80 mm × 10 mm × 4 mm. The samples were conditioned for 2 d and the test was conducted at 23 °C ± 2 °C

and $50\% \pm 5\%$ RH. Mantia and Morreale (2007) studied the effect of introducing PP into a polypropylene-wood flour composite, and found that an increase in the impact strength was observed for the un-notched samples, while no remarkable improvement was observed in the impact strength of the notched samples. Based on this finding, un-notched specimens were selected for the impact test.

Morphological properties analyses

Samples broken in the impact tests were used for the scanning electron microscopy (SEM) analysis. The SEM analysis was conducted *via* an ultra-high-resolution scanning electron microscope (FESEM) (Hitachi-SU 8000, Tokyo, Japan) to study and observe the morphology of the composite, determine the silica content on the surface and inside the KBF, and to measure the size of the voids inside the wood and the size of the silica that filled the voids. The samples were first coated with platinum to make them more conductive.

Energy dispersive X-ray (EDX) analysis, conducted as an elemental analysis at the end, was also vital in determining the percentages of the components in the measured area, which were used for identification purposes. The size of the silica was determined using Image J software (Rueden *et al.* 2017). About 100 measurements were recorded of each condition were used in the representative images of the SEM, as reported by Raabe *et al.* (2014).

Fourier transform infrared spectroscopy

Fourier transform infrared (FTIR) spectroscopy was conducted using a Nicolet i10s FTIR (Thermo Electron Scientific Instruments LLC, Waltham, MA, USA) equipped with attenuated total reflection to observe the morphology of the composite and silica content present on the surface and inside the KBF.

The spectral range used was 4000 cm^{-1} to 500 cm^{-1} at a resolution of 2 cm^{-1} at room temperature. The data obtained were recorded in the transmittance mode according to ASTM E168 (2016).

Computed tomography (CT) scan

The X-ray computed tomography (CT) scan analysis was conducted using a Scando Medical μ CT 40 (Brüttisellen, Switzerland) to observe the morphology of the hybrid composite and void content present on the surface and inside the system. The test was performed with a minimum of three samples that had the dimensions $40\text{ mm} \times 10\text{ mm} \times 4\text{ mm}$. The samples were subjected to X-ray source and detector pair rotated resulting in projection image throughout 360° rotation. Micro CT is a well-known technique to study the interior features of solid objects without destroying the object. The test was performed in accordance with ASTM E1695-95 (2013) to obtain digital information of the composites in 3-D.

Thermal properties test

The thermal properties were analyzed by thermogravimetric analysis (TGA) using a Mettler Toledo thermogravimetric analyzer (model 851e, Columbus, OH, USA) with nitrogen and purified air. The samples were dried for 2 h at 100°C prior to the test to minimize the effects of moisture. The sample weight was approximately 10 mg to 13 mg. The samples were heated at a constant heating rate of $10^\circ\text{C}/\text{min}$ from 30°C to 800°C with a nitrogen purge and heated from 800°C to 1000°C with an air purge. The

maximum inflection points were determined from the temperature at the maximum peak of the TGA curves.

RESULTS AND DISCUSSION

Preparation of *in situ* Sol-gel Silica-modified Kenaf Bast Fiber (KBF-S)

It was observed that the silica content in the KBF-S was 20.40 wt.%. The silica content in the KBF-S was analyzed with a burn test and TGA. A 1.1% residue of KBF was found after burning the KBF at 600 °C for 6 h. The total burn off of the untreated KBF was 98.9%. The residue content was 19.20% for KBF-S. Thus, the silica content was determined as 18.1%.

When modifying the KBF with the *in situ* sol-gel silica process, a thin layer can be formed between the butylamine molecules and the KBF *via* hydrogen bonding, which prevents the KBF hydroxyl groups from participating in the TEOS to silica reaction (Pena *et al.* 2016). This was visualized in the SEM images of the untreated KBF and KBF-S, which are shown in Fig. 1. The SEM image of the KBF revealed the presence of voids and the absence of silica on the surface (Fig. 1a). The SEM image of KBF-S revealed the surface was partially covered with silica and the voids were filled with silica particles. The size of the silica ranged from 0.15 µm to 0.20 µm in diameter.

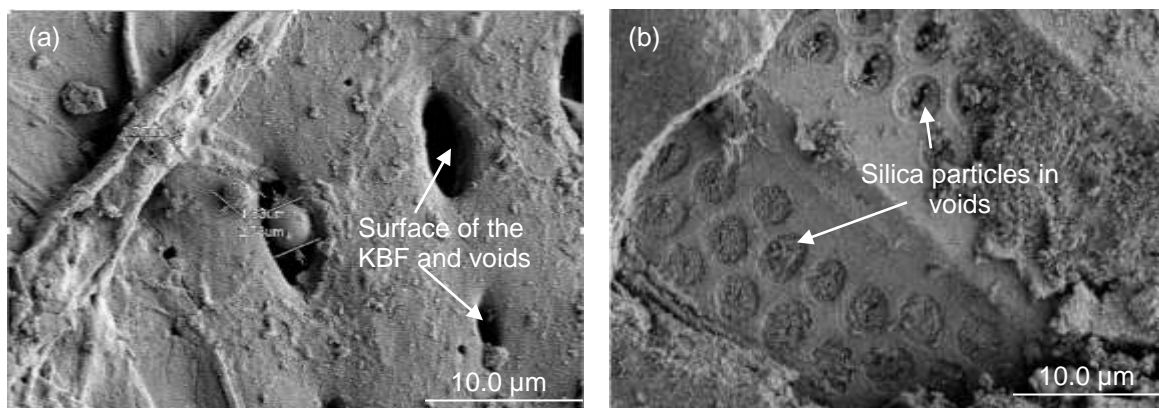


Fig. 1. SEM images of the KBF (a) and KBF-S (b)

Figure 2 shows the elemental analysis with EDX of the KBF and KBF-S. Both elemental readings were specifically conducted to focus on the void area of the fiber. It was found that carbon (C), oxygen (O), and platinum (Pt) were present in the KBF. The presence of Pt was due to the coating present in the void. For the KBF-S, the elemental analysis revealed the presence of C, O, Pt, and silica (Si). It was found there was a higher concentration of Si present in the focused area (39.86 wt.%) compared with the other components. Furthermore, the presence of chlorine (Cl) in KBF might have happened naturally, as there was no chemical used that contained Cl. From these EDX findings and SEM results, the presence of silica in the void areas of the KBF-S and surrounding surface was demonstrated.

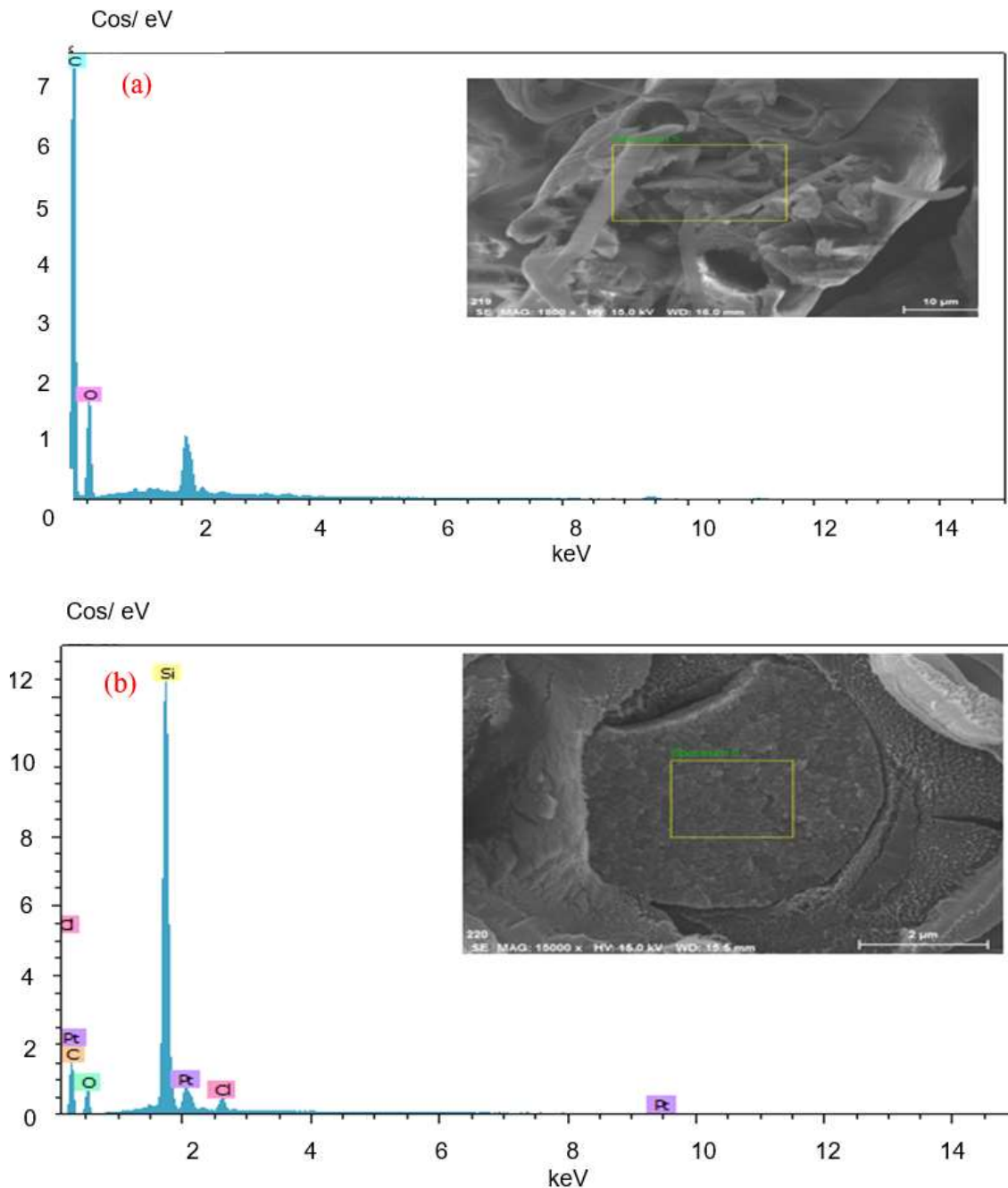


Fig. 2. Elemental analysis of the KBF (a) and KBF-S (b)

The formation of chemical bonds between the silica and kenaf can be established indirectly and qualitatively by FTIR analyses. The results of the FTIR analysis are presented in Table 1. It is worth noting that there are several noticeable bands that are important in determining the presence and absence of silica, as well as the reduction of the hemicellulose and lignin contents in the KBF-S. The broad band from 3100 cm^{-1} to 3500 cm^{-1} that was attributed to the -OH stretching of moisture and the peak at 2898 cm^{-1} caused by C-H stretching were present in all three samples, but the -OH groups had a lower intensity in both KBF-S samples compared with the untreated KBF. According to Abdul Khalil *et al.* (2010), a decrease in the intensity of the -OH groups for KBF-S

indicated that the content of -OH groups was reduced. The untreated KBF exhibited a broader peak of the -OH at 3333 cm^{-1} compared with the KBF-S, which indicated a decrease in -OH groups in the sol-gel silica-treated fibers. A familiar stretched C=O peak at 1635 cm^{-1} was present in the KBF, and this indicated the presence of acetyl esters in the hemicellulose and carbonyl aldehydes in the lignin. This peak was comparatively reduced in the KBF-S. This was caused by the butylamine treatment of the KBF. This treatment has the same effect as any alkali treatment on the fibers, and lessened the hemicellulose and lignin contents in the fiber, but did not eliminate them completely (Asumani *et al.* 2012). The presence of lignin in the KBF was made evident by a peak at 1245 cm^{-1} , which disappeared in the KBF-S (Razak *et al.* 2014). The sol-gel silica treatment of KBF led to a decrease in peak frequencies of two major regions in the KBF-S compared with the untreated KBF. The first region was 1310 cm^{-1} to 1330 cm^{-1} , which indicated a reduction in the C-OH bonds in the KBF-S. This phenomenon suggested that C-O-Si bonds were formed. The second major region was 1000 cm^{-1} to 800 cm^{-1} , which showed major silica bands detected in the KBF-S, but an absence in the untreated KBF. This was attributed to the stretching vibrations of Si-O-Si and Si-O-C (Bandyopadhyay *et al.* 2005). The presence of these peaks (1310 cm^{-1} to 1330 cm^{-1} and 1000 cm^{-1} to 800 cm^{-1}) suggested that chemical bonds between the cellulose and silica were formed after the modification of the KBF.

Table 1. FTIR Wavelengths of the KBF and KBF-S

Assignments	FTIR Wavelengths (cm^{-1})		
	TEOS	KBF	KBF-S
ν_s Si-O-Si O-Si-CH ₃	800	-	792
ν_{as} Si-O-Si	1050	-	1055
C-O vibration	-	1245	-
C-OH	-	1316	Reduction
Carbonyl (C=O)	-	1635	Reduction
C-H aliphatic	-	2916	2898
-OH stretching	3450	3332	3331

Characterization of the PP-KBF and PP-KBF-S Composites

To determine the effect of the silica, in the form of KBF-S, on the properties of the PP-based composites, the PP-KBF and PP-KBF-S composites were comparatively evaluated. Analyses were conducted that determined the mechanical properties, void content, thermal properties, and morphology of the composites. The KBF and KBF-S content in the composites was 30 wt.%.

Determination of the physical properties

The specific gravity (ρ) and void content of the PP-KBF and PP-KBF-S composites were determined and are given in Table 2. The porosity of the KBF might have caused air or moisture to be trapped in it, which in turn caused the formation of voids in the composite during mixing (Akil *et al.* 2010). It was found that the PP-KBF showed a higher void content compared with the PP-KBF-S. Because of the presence of silica, which filled up the voids as was discussed earlier, the KBF-S was more compact



and packed. Consequently, the density of the PP-KBF-S and the PP-KBF were almost similar. The presence of silica reduced the void content by approximately 60%.

Table 2. Specific Gravity and Void Content of the PP-KBF and PP-KBF-S Composites

Sample	Theoretical Specific Gravity ρ (g/cm ³)	Measured Specific Gravity ρ (g/cm ³)	Void Content (%)
PP-KBF	1.02	1.009	1.17
PP-KBF-S	1.03	1.022	0.77

Silica decreasing the void content in the PP-KBF-S was further evidenced through the quantitative CT scan on the PP-KBF and PP-KBF-S samples. The results of the scan are presented in Table 3. A direct 3-D morphometric analysis of the cross-sectional area of the PP-KBF-S indicated a relative bone volume (BV/TV) of 82%, which was higher compared with the 54% BV/TV value found for the PP-KBF. In terms of producing a composite with an acceptable efficacy, the presence of silica in the PP-KBF-S system provided a 32% improvement compared with the PP-KBF. Amiri (2016) also studied the differences between conventional void fractions and bio-based resin-flax composites with advanced micro CT scans, and they were found to differ by 1% to 7%.

Table 3. Morphometric Analysis of the Cross-sectional Areas of the PP-KBF and PP-KBF-S

	PP-KBF	PP-KBF-S
Feature		
Mean / Density [1/cm] of -TV (Apparent) -BV (Material)	0.4180 0.560	0.4891 0.564
Relative bone volume BV/TV Value	0.5481	0.8294

Morphological properties of the PP-KBF and PP-KBF-S

The morphology analysis was conducted using SEM image analysis of the PP-KBF and PP-KBF-S composites to identify the presence of silica particles and whether silica formed inside the voids of the composites. These images are presented in Fig. 3. The SEM image of the PP-KBF-S showed that the silica filled the surface and voids of the kenaf fiber in the composite (Fig. 3b). Figure 3a clearly shows the presence of voids. The voids acted as crack initiation points, which evidently contributed to the low mechanical properties of the PP-KBF composites. The surface was covered with silica and the voids were filled with silica particles. The size of the silica was measured and found to range from 3.36 μm to 3.59 μm and 2.5 μm to 3.07 μm for that on the surface and in the voids, respectively. The presence of silica increased the hydrophobicity of the kenaf fiber, which was probably why the hydrophobic PP had more inconsistent mechanical properties.

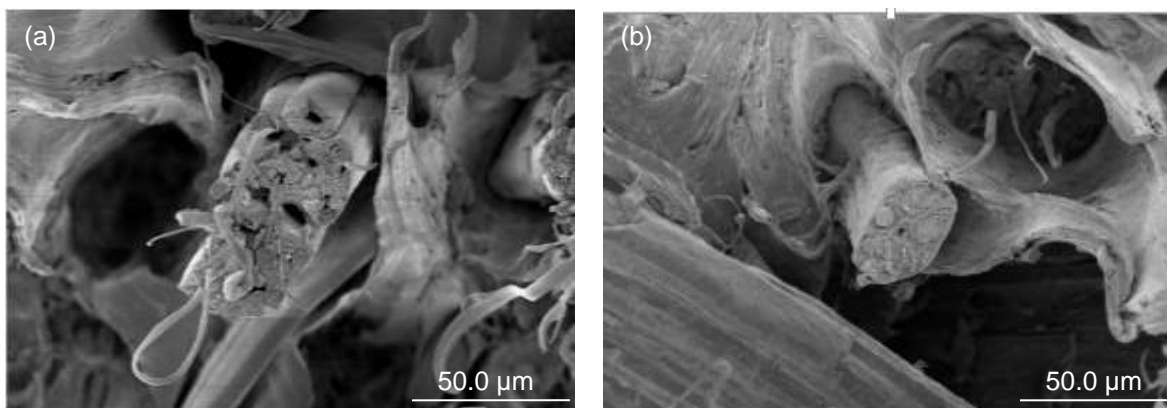


Fig. 3. SEM images of the PP-KBF (a) and PP-KBF-S (b) composites

Mechanical properties of the PP-KBF and PP-KBF-S

Table 4 shows the measured tensile properties, which were the tensile strength, Young's modulus, and extension at maximum stress, of the PP-KBF and PP-KBF-S composites. It was observed that the tensile strength and extension at maximum stress were slightly higher in the PP-KBF-S, but the Young's modulus of the PP-KBF-S composite was lower when compared with the PP-KBF composite. The PP-KBF-S and PP-KBF had comparable values for the tensile strength and extension at maximum stress. The PP-KBF-S had a tensile strength and extension at maximum stress of 29.6 MPa and 2.45 mm, respectively. For the PP-KBF composite, the tensile strength and extension at maximum stress were 29.0 MPa and 2.40 mm, respectively. The Young's modulus values were 1141 MPa and 1391 MPa for the PP-KBF and PP-KBF-S composites, respectively. This increase in the Young's modulus was most likely because of the presence of chemical interactions between the PP and KBF-S, which was slightly polar due to the presence of silica (Bajuri *et al.* 2016). A similar observation was reported by Tay *et al.* (2012), who observed an increase in the Young's Modulus after the chemical modification of kenaf fiber using silica-based montmorillonite.

Table 4. Tensile Properties of the PP-KBF and PP-KBF-S Composites

Samples	Tensile Strength (MPa)	Young's Modulus (MPa)	Extension at Maximum Stress (mm)
PP-KBF	29.0±2.9	1391±148.7	2.40±0.3
PP-KBF-S	29.6±1.3	1141±193.7	2.45±0.6

Table 5 shows the flexural properties values measured for the PP-KBF and PP-KBF-S composites, specifically the flexural strength and modulus. The PP-KBF-S had a flexural strength of 45.04 MPa, which was noticeably higher than that of the PP-KBF (33.2 MPa). This observation was probably related to the mode of deformation in the flexural test, which involved tension, compression, and shear forces. Because the PP-KBF-S was denser than the PP-KBF, *i.e.* less voids, more compression and shear forces were required to deform the material, especially at higher degrees of deformation. Similar findings were reported by Bajuri *et al.* (2016), who observed that the presence of nano-silica enhanced the flexural strength of a kenaf-epoxy composite. Unlike the Young's modulus, the flexural modulus decreased in the PP-KBF composite (2451 MPa) when

compared with that of the PP-KBF-S composite (2650 MPa). Tay *et al.* (2012) also reported that the decreased flexural properties of the kenaf-PP composite with the addition of silica-based montmorillonite clay to the kenaf-PP was because of an incompatibility of the hydrophilic silica and kenaf and the hydrophobic PP. The impact strengths of the PP-KBF and PP-KBF-S were 9.7 J/m and 12.3 J/m, respectively. A higher impact strength enhanced the ability of the material to absorb mechanical energy during deformation and fracture under impact loading. In the case of the PP-KBF-S, the probable explanation for this was that the energy absorbed by the matrix was transferred to the silica particles, which increased the impact strength (Bajuri *et al.* 2016).

Table 5. Flexural Properties of the PP-KBF and PP-KBF-S Composites

Samples	Flexural Strength (MPa)	Flexural Modulus (MPa)	Impact Strength (J/m)
PP-KBF	33.21±1.6	2451±28.2	9.7±0.6
PP-KBF-S	45.02±3.6	2650±25.3	12.3±1.0

The PP-KBF-S composite had a similar tensile strength, better flexural and impact strengths, and inconsistent Young's and flexural moduli when compared with the PP-KBF composite. The improvement of the mechanical properties for these composites were suspect, unstable, and there was probably no chemical interaction because both silica and KBF are polar, while PP is non-polar. The improvement in the mechanical properties was confirmed *via* the tensile strength obtained from the void content measurement and morphometric analysis using the micro CT scan of the PP-KBF and PP-KBF-S. As was expected, the PP-KBF-S had a lower void content because of the formation of silica in the voids during the sol-gel silica process. In the study by Dobreva *et al.* (2006), it was mentioned that the unmodified wood flour had a large amount of voids, which in turn caused the brittle fracture of the matrix, debonding, and pulling out of wood flour particles from the PP matrix, and resulted in low mechanical properties. Generally, the presence of voids in the composite acted as weak points, which caused poor mechanical properties.

Thermal analysis of the PP-KBF and PP-KBF-S composites

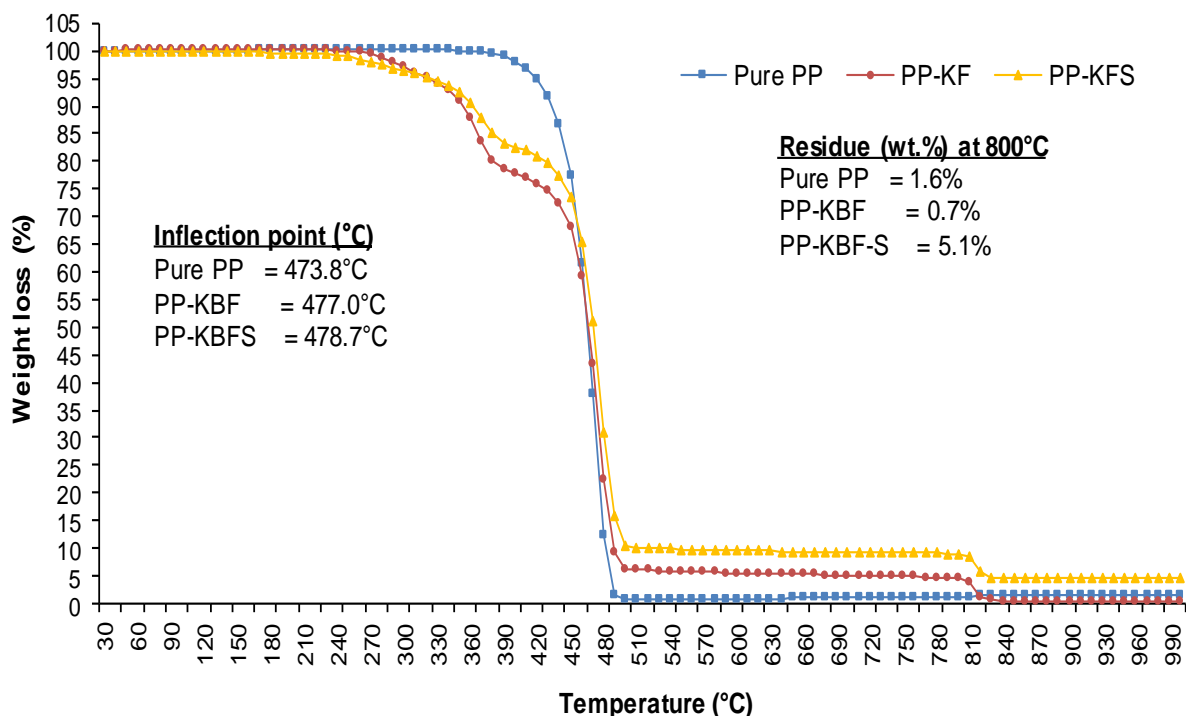
The thermal properties of the PP, PP-KBF composite, and PP-KBF-S composite were determined for the weight losses of 2 wt.% to 30 wt.%. This is presented in Fig. 4, and the data that were obtained are summarized in Table 6. It was determined that the PP-KBF-S had the highest thermal properties because of the sol-gel silica modification, which resulted in the composite having a better thermal resistance. At a 2% weight loss for the pure PP, decomposition started later (401.1 °C) than for the PP-KBF and PP-KBF-S, which started at 285.0 °C and 270.4 °C, respectively. The PP has long hydrocarbon chains, which caused the higher degradation temperature, while the PP-KBF and PP-KBF-S consisted of kenaf fibers that are more sensitive to an increasing temperature. Rimdusit *et al.* (2011) studied the thermal decomposition behavior of wood flour, which degraded at lower temperatures than the PP in their composite system. This indicated that the presence of KBF in the PP composite decreased the decomposition temperature compared with the pure PP.

Table 6. Thermogravimetric Analysis Data of the PP, PP-KBF, and PP-KBF-S

Sample	Decomposition Temperature (T_d , °C) at Different Weight Losses (%)					Residue (wt.%) at 800 °C	Inflection Point (°C)
	2	5	10	20	30		
PP	401.1	419.9	433.6	447.3	454.7	1.6	473.8
PP-KBF	285.0	309.8	338.8	365.5	393.0	0.7	477.0
PP-KBF-S	270.4	324.9	362.3	428.1	454.1	5.1	478.7

In comparison, the presence of silica in the PP-KBF-S increased the decomposition temperature for the 5%, 10%, 20%, and 30% weight losses. Therefore, the PP-KBF-S composites were more thermally stable and had higher starting temperatures for decomposition compared with the PP-KBF. The silica might have acted as a thermal retarding agent in the composite. The inflection point increased by 1.2 °C and 3.6 °C in the PP-KBF-S compared with the PP-KBF and PP, respectively.

Figure 4 showed that the pure PP required higher temperatures to be degraded (400 °C to 500 °C). The curve of the PP-KBF-S shifted to the right towards higher temperatures when compared with the PP-KBF. The difference in decomposition temperatures between the PP-KBF and PP-KBF-S was because of the composition (hemicellulose, cellulose, and lignin) and the addition of silica in the PP-KBF-S. At the 1st slope, the 2% to 30% weight loss occurred from 250 °C to 320.9 °C for the PP-KBF and from 220.4 °C to 412.2 °C for the PP-KBF-S, during which the composites underwent thermal degradation of the cellulose and hemicellulose.

**Fig. 4.** Thermogravimetric curves of the PP, PP-KBF composite, and PP-KBF-S composite

At the 2nd slope, the weight loss was because of the decomposition of lignin from 380 °C to 490 °C for the PP-KBF and from 410 °C to 520 °C for the PP-KBF-S. Therefore, it was concluded that the presence of silica increased the degradation

temperature and improved the thermal stability of the PP-KBF-S. The degradation temperatures of the composites were similar to those reported by Jeske *et al.* (2012), who found that wood flour degradation generally occurred over the wide temperature range of 250 °C to 600 °C. Their study also indicated that cellulose and hemicellulose degraded at 200 °C to 450 °C, while lignin decomposed at 250 °C to 500 °C. For the residual weight (%), the PP-KBF-S had a higher residue than the PP-KBF and PP. This was caused by the presence of silica. Similarly, Wu and Liao (2008) observed a higher residue yield of PLA-g-AA/SiO₂ nanocomposites, which contained silica that acted as a physical barrier.

CONCLUSIONS

1. The silica content in the KBF-S was 20.40 wt.%. The morphological analyses of the KBF-S revealed that the surface was covered with silica, and the voids were filled with silica particles. The size of the silica ranged from 0.15 µm to 0.20 µm.
2. The PP-KBF had a higher void content compared with the PP-KBF-S. The presence of silica reduced the void content by approximately 60%.
3. The morphology analysis of the PP-KBF and PP-KBF-S composites revealed that silica formed in the sol-gel silica process, which occurred inside the voids of the composites.
4. Determination of the mechanical properties showed that the tensile strength and extension at maximum stress were higher in the PP-KBF-S, but the Young's modulus of the PP-KBF-S composite was lower, when compared with the PP-KBF composite. Unlike the Young's modulus, the flexural modulus was found to have increased in the PP-KBF-S composite (2650 MPa) when compared with that of the PP-KBF composite (2451 MPa).
5. The PP-KBF-S had the highest thermal properties because of the sol-gel silica modification, which caused the composite to have a better thermal resistance. The presence of silica reduced the degradation temperature and improved the thermal stability of the PP-KBF-S, when compare with PP and PP-KBF.

ACKNOWLEDGMENTS

The authors would like to thank the Universiti Kuala Lumpur and Majlis Amanah Rakyat (MARA) for the financial support through the Short Term Research Grant (STRG 015 Universiti Kuala Lumpur) and Skim Geran Penyelidikan dan Inovasi MARA (SGPIM 1/33/04/01/15 (4) MARA), respectively.

REFERENCES CITED

- Abdul Khalil, H. P. S., Davoudpour, Y., Saurabh, C. K., Hossain, M. S., Adnan, A. S., Dungani, R., Paridah, M. T., Sarker, M. Z. I., Faita, M. R. N., Syakir, M. I., *et al.* (2016). "A review on nanocellulosic fibres as new material for sustainable packaging:

- Process and applications,” *Renew. Sust. Energ. Rev.* 64, 823-836. DOI: 10.1016/j.rser.2016.06.072
- Abdul Khalil, H. P. S., Yusra, A. F. I., Bhat, A. H., and Jawaid, M. (2010). “Cell wall ultrastructure, anatomy, lignin distribution, and chemical composition of Malaysian cultivated kenaf fiber,” *Ind. Crop. Prod.* 31(1), 113-121. DOI: 10.1016/j.indcrop.2009.09.008
- Akil, H. M., de Rosa, I. M., Santulli, C., and Sarasini, F. (2010). “Flexural behaviour of pultruded jute/glass and kenaf/glass hybrid composites monitored using acoustic emission,” *Mat. Sci. Eng. A-Struct.* 527(12), 2942-2950. DOI: 10.1016/j.msea.2010.01.028
- Amiri, A. (2016). “Advanced method for void fraction evaluation of natural fiber composites using micro-Ct technology,” in: *SAMPE Conference Proceedings*, Long Beach, CA.
- ASTM D790-17 (2017). “Standard test methods for flexural properties of unreinforced and reinforced plastics and electrical insulating materials,” ASTM International, West Conshohocken, PA.
- ASTM D3039 (2014). “Standard test method for tensile properties of polymer matrix composite materials,” ASTM International, West Conshohocken, PA.
- ASTM E168 (2016). “Standard practices for general techniques of infrared quantitative analysis,” ASTM International, West Conshohocken, PA.
- ASTM E1695-95 (2013). “Standard test method for measurement of computed tomography (CT) system performance,” ASTM International, West Conshohocken, PA.
- Asumani, O. M. L., Reid, R. G., and Paskaramoorthy, R. (2012). “The effects of alkali-silane treatment on the tensile and flexural properties of short fibre non-woven kenaf reinforced polypropylene composites,” *Compos. Part A-Appl. S.* 43(9), 1431-1440. DOI: 10.1016/j.compositesa.2012.04.007
- Bajuri, F., Mazlan, N., Ishak, M. R., and Imatomi, J. (2016). “Flexural and compressive properties of hybrid kenaf/silica nanoparticles in epoxy composite,” *Procedia Chemistry* 19, 955-960. DOI: 10.1016/j.proche.2016.03.141
- Bismarck, A., Baltazar-Y-Jimenez, A., and Sarikakis, K. (2006). “Green composites as panacea? Socio-economic aspects of green materials,” *Environ. Dev. Sustain.* 8(3), 445-463. DOI: 10.1007/s10668-005-8506-5
- Bounor-Legaré, V., and Cassagnau, P. (2014). “*In situ* synthesis of organic-inorganic hybrids or nanocomposites from sol-gel chemistry in molten polymers,” *Prog. Polym. Sci.* 39(8), 1473-1497. DOI: 10.1016/j.progpolymsci.2014.04.003
- Bourmaud, A., and Baley, C. (2007). “Investigations on the recycling of hemp and sisal fibre reinforced polypropylene composites,” *Polym. Degrad. Stabil.* 92(6), 1034-1045. DOI: 10.1016/j.polymdegradstab.2007.02.018
- Davoudpour, Y., Hossain, S., Khalil, H. P. S. A., Haafiz, M. K. M., Ishak, Z. A. M., Hassan, A., and Sarker, Z. I. (2015). “Optimization of high pressure homogenization parameters for the isolation of cellulosic nanofibers using response surface methodology,” *Ind. Crop. Prod.* 74, 381-387. DOI: 10.1016/j.indcrop.2015.05.029
- Dobrova, D., Nenkova, S., and Vasileva, S. (2006). “Morphology and mechanical properties of polypropylene-wood flour composites,” *BioResources* 1(2), 209-219. DOI: 10.15376/biores.1.2.209-219

- Hashim, A. S., Kohjiya, S., and Ikeda, Y. (1995). "Moisture cure and *in situ* silica reinforcement of epoxidized natural rubber," *Polymer International* 38(2), 111-117. DOI: 10.1002/pi.1995.210380202
- Hubbe, M., Rojas, O., and Lucia, L. (2015). "Green modification of surface characteristics of cellulosic materials at the molecular or nano scale: A Review," *BioResources* 10(3), 6095-6206. DOI: 10.15376/biores.10.3.Hubbe
- Ikeda, Y., and Kameda, Y. (2004). "Preparation of "green" composites by the sol-gel process: *In situ* silica filled natural rubber," *J. Sol-Gel Sci. Techn.* 31(1), 137-142. DOI: 10.1023/B:JSST.0000047975.48812.1b
- Ireana Yusra, A., Abdul Khalil, H., Hossain, M. S., Davoudpour, Y., Astimar, A. A., Zaidon, A., Dungani, R., and Mohd Omar, A. K. (2015). "Characterization of plant nanofiber-reinforced epoxy composites," *BioResources* 10(4), 8268-8280. DOI: 10.15376/biores.10.4.8268-8280
- ISO 179 (2010). "Determination of Charpy impact properties – Part 1: Non-instrumented impact test," International Organization for Standardization, Geneva, Switzerland.
- Jeske, H., Schirp, A., and Cornelius, F. (2012). "Development of a thermogravimetric analysis (TGA) method for quantitative analysis of wood flour and polypropylene in wood plastic composites (WPC)," *Thermochimica Acta* 543(Supplement C), 165-171. DOI: 10.1016/j.tca.2012.05.016
- Lambert, A. J. D., and Gupta, S. M. (2004). *Disassembly Modeling for Assembly, Maintenance, Reuse and Recycling*, CRC Press, Boca Raton, FL.
- Mantia, F. P. L., and Morreale, M. (2007). "Improving the properties of polypropylene-wood flour composites by utilization of maleated adhesion promoters," *Composite Interfaces* 14(7-9), 685-698. DOI: 10.1163/156855407782106500
- Owolabi, A. F., Haafiz, M. K. M., Hossain, M. S., Hussin, M. H., and Fazita, M. R. N. (2017). "Influence of alkaline hydrogen peroxide pre-hydrolysis on the isolation of microcrystalline cellulose from oil palm fronds," *Int. J. Biol. Macromol.* 95, 1228-1234. DOI: 10.1016/j.ijbiomac.2016.11.016
- Raabe, J., de Souza Fonseca, A., Bufalino, L., Ribeiro, C., Martins, M. A., Marconcini, J. M., and Tonoli, G. H. D. (2014). "Evaluation of reaction factors for deposition of silica (SiO₂) nanoparticles on cellulose fibers" *Carbohydrate Polymers*, 114(Supplement C), 424-431. DOI: 10.1016/j.carbpol.2014.08.042
- Razak, N., Ibrahim, N., Zainuddin, N., Rayung, M., and Saad, W. (2014). "The influence of chemical surface modification of kenaf fiber using hydrogen peroxide on the mechanical properties of biodegradable kenaf fiber/poly(lactic acid) composites," *Molecules* 19(3), 2957-2968. DOI: 10.3390/molecules19032957
- Rimdit, S., Smittakorn, W., Jittarom, S., and Tiptipakorn, S. (2011). "Highly filled polypropylene rubber wood flour composites," *Engineering Journal* 15, 17-30.
- Rosamah, E., Hossain, M. S., Abdul Khalil, H. P. S., Wan Nadirah, W. O., Dungani, R., Nur Amiranajwa, A. S., Suraya, N. L. M., Fizree, H. M., and Mohd Omar, A. K. (2017). "Properties enhancement using oil palm shell nanoparticles of fibers reinforced polyester hybrid composites," *Adv. Compos. Mater.* 26(3), 259-272. DOI: 10.1080/09243046.2016.1145875
- Rueden, C. T., Schindelin, J., Hiner, M. C., DeZonia, B. E., Walter, A. E., Arena, E. T., and Eliceiri, K. W. (2017). "ImageJ2: ImageJ for the next generation of scientific image data". *BMC Bioinformatics* 18(1), 529. DOI: 10.1186/s12859-017-1934-z.
- Peña, L. F., Nanayakkara, C. E., Mallikarjunan, A., Chandra, H., Xiao, M., Lei, X., Pearlstein, R. M., Derecskei-Kovacs, A., and Chabal, Y. J. (2016). "Atomic layer

- deposition of silicon dioxide using aminosilanes di-sec-butylaminosilane and bis(tert-butylamino)silane with ozone,” *The Journal of Physical Chemistry C* 120(20), 10927-10935. DOI: 10.1021/acs.jpcc.6b01803
- Saad, M. J. (2012). “The effect of maleated polypropylene (MAPP) on the mechanical properties of kenaf core - polypropylene composites,” *Journal of Sustainability Science and Management* 7(1), 49-55.
- Saba, N., Paridah, M. T., and Jawaid, M. (2015). “Mechanical properties of kenaf fibre reinforced polymer composite: A review,” *Constr. Build. Mater.* 76, 87-96. DOI: 10.1016/j.conbuildmat.2014.11.043
- Tajeddin, B., Rahman, R. A., and Abdulah, L. C. (2010). “The effect of polyethylene glycol on the characteristics of kenaf cellulose/low-density polyethylene biocomposites,” *Int. J. Biol. Macromol.* 47(2), 292-297. DOI: 10.1016/j.ijbiomac.2010.04.004
- Tawakkal, I. S. M. A., Cran, M. J., and Bigger, S. W. (2014). “Effect of kenaf fibre loading and thymol concentration on the mechanical and thermal properties of PLA/kenaf/thymol composites,” *Ind. Crop. Prod.* 61, 74-83. DOI: 10.1016/j.indcrop.2014.06.032
- Tay, G. S., Azniwati, A. A., Azizah, A. B., Rozman, H. D., and Musa, L. (2012). “The flexural and impact properties of kenaf-polypropylene composites filled with montmorillonite filler,” *Polym.-Plast. Technol.* 51(2), 208-213. DOI: 10.1080/03602559.2011.625376
- Thakur, V. K., and Thakur, M. K. (2014). “Processing and characterization of natural cellulose fibers/thermoset polymer composites,” *Carbohydr. Polym.* 109, 102-117. DOI: 10.1016/j.carbpol.2014.03.039
- Yang, H., Peng, Z., Zhou, Y., Zhao, F., Zhang, J., Cao, X., and Hu, Z. (2011). “Preparation and performances of a novel intelligent humidity control composite material,” *Energ. Buildings* 43(2-3), 386-392. DOI: 10.1016/j.enbuild.2010.10.001

Article submitted: September 4, 2017; Peer review completed: December 16, 2017;
Revised version received and accepted: January 5, 2018; Published: January 30, 2018.
DOI: 10.15376/biores.13.1.1977-1992